

# Platinum–Dendrimer Nanocomposite Films on Gold Surfaces for Electrocatalysis

S. Raghu · R. G. Nirmal · J. Mathiyarasu ·  
Sheela Berchmans · K. L. N. Phani · V. Yegnaraman

Received: 15 May 2007 / Accepted: 3 June 2007 / Published online: 23 June 2007  
© Springer Science+Business Media, LLC 2007

**Abstract** In this communication, we report a strategy for the preparation of Pt nanoparticles encapsulated in Generation 4.5 (Polyamido amine) PAMAM dendrimer and subsequent chemical linking of the nanocomposite to the gold electrode through a self assembled cystamine monolayer. The modification resulted in the formation of a robust electrochemically active thin film with very high surface area, reflected by the enhanced hydrogen adsorption coverage. Interestingly, TEM images revealed self-assembly of Pt nanoparticles and the SAED (Selected Area Electron Diffraction) patterns showed the presence of Pt single crystals (111). The Pt-dendrimer nanocomposite film obtained using the novel modification procedure exhibited high electrocatalytic activity for the oxidation of organic fuels like methanol, ethanol and ethylene glycol. The film did not suffer from degradation even after repeated use in solution-phase voltammetry. It is however observed that the intermediate SAM layer and the bulky PAMAM dendrimer (generation 4.5) have slowed down the electron transfer kinetics which is reflected by a relatively high overpotential for methanol oxidation. Nevertheless this shortcoming is more than compensated by the existence of Pt(111) planes, which alleviate CO poisoning.

**Keywords** Dendrimers · Platinum–dendrimer nanocomposite · Electrocatalysis · Self-assembly · Cystamine · Template synthesis

## 1 Introduction

Recently, synthesis of nanostructured materials with high surface area has received significant interest since these materials possess unique properties and lend themselves to a number of impressive applications in catalysis, fuel cells and chemical sensors [1–5]. Nanostructured Pt materials have excellent catalytic properties and preparation of electrocatalysts incorporating these materials is a contemporary and challenging task. In this communication, we report the synthesis of high surface area Pt nanoparticles encapsulated by dendrimers and a novel strategy for linking the dendrimers to the electrode surface to yield robust, electrocatalysts.

Dendrimers are outstanding candidates for template synthesis of nanoparticles because of their regular structure and chemical versatility [6]. The terminal functional groups serve as handles to facilitate surface immobilization. Dendrimer-encapsulated nanoparticles can be nearly monodisperse. Though they are passive against aggregation, major part of the surface is free for them to be catalytically active [7–13]. The synthesis and characterization of dendrimer-encapsulated monometallic Pd and Pt clusters and their use as catalysts for hydrogenation, oxygen reduction and Heck coupling reaction have been reported [6]. Recently, dendrimer-encapsulated Pd–Pt catalyst was found to exhibit a cooperative effect, which is attributed to the presence of bimetallic nanoparticles [14–17]. Core-shell bimetallic nanoparticles are interesting models for the formation of alloys at angstrom scale. In all these cases, hydroxyl and amine terminated dendrimers were employed. In view of their functional advantages, dendrimer molecules, mostly utilized for solution-phase reactions, offer themselves as apt candidates for immobilization on electrode surfaces to yield enhanced electroactivity

S. Raghu · R. G. Nirmal · J. Mathiyarasu · S. Berchmans (✉) ·  
K. L. N. Phani · V. Yegnaraman  
Electrodes and Electrocatalysis Division, Central  
Electrochemical Research Institute, Karaikudi 630006, India  
e-mail: sheelaberchmans@yahoo.com

[18–20]. PAMAM dendrimers of generation 3.5, 4.5 and 5.5 have been used to prepare nanocomposites by encapsulating nanoparticles of Au and bimetallic Au/Ag [21–24]. Dendrimer-encapsulated Au nanoparticles exhibit antioxidant properties and the bimetallic Au/Ag nanoparticles catalyse the reduction of *p*-nitrophenol. Recently, Pt nanoparticles have been encapsulated into dendrimer of generation 4.5, but neither catalytic activity nor the existence of single crystal nature of the encapsulated Pt particles has been reported [25]. Kim et al. [26] have reported the preparation of platinum–dendrimer hybrid nanowires using alumina templates, which exhibited electrocatalytic properties. In a recent study [27], we have shown fourth-generation amine-terminated PAMAM dendrimer to serve as adhesion agent to deposit nanoparticulate thin films of Pt on Au. These films exhibited significantly enhanced electrocatalytic activity towards methanol oxidation.

In the present study, the preparation of Pt nanoparticles encapsulated in carboxyl-terminated generation 4.5 PAMAM dendrimer (G-4.5) and its chemical linking to the electrode for obtaining electrocatalytic surfaces are described. G-4.5 is characterized by the presence of an ethylenediamine core, 128 carboxyl groups as anchors and 126 tertiary amine groups for complexation and is readily amenable to a variety of chemical functionalization schemes. The relatively high density of tertiary amine groups in G-4.5 ensures incorporation of a large number of metal particles while the dendrimer still remains sufficiently “open” for the reactant species to access metal particles. The terminal carboxyl groups facilitate stabilization of the nanoparticles through inter-dendrimer hydrogen bonding. It has been demonstrated that control of pH around 8 during borohydride reduction leads to the formation of metal nanoclusters without aggregation [24, 6]. Further, linking of these nanoparticle-loaded dendrimers to the electrode has been attempted by a novel way of electrode modification involving diazotization reaction, for which the amine groups of the cystamine monolayer on Au served as the platform. The carboxyl-terminated dendrimer is tethered to Au surface through ester linkages [28] established between the diazotized cystamine monolayer and the dendrimer. The electrocatalytic activity of encapsulated Pt nanoparticles is demonstrated for the oxidation of small molecules like methanol, ethanol and ethylene glycol.

## 2 Experimental

The following chemicals were used as received: PAMAM dendrimer, G-4.5, (Aldrich),  $K_2PtCl_4$  (Merck), sodium borohydride, cystamine dihydrochloride (Aldrich), sodium nitrite (Merck).

### 2.1 Preparation of Pt-dendrimer Nanocomposite

A solution of 0.125 mM of PAMAM dendrimer (G-4.5) is mixed with 10 mM  $K_2PtCl_4$  in water and kept stirred for several days under cold conditions. The pH is maintained slightly alkaline (~8 pH). Then,  $PtCl_4^{2-}$  is reduced by adding a few drops of 0.1 M sodium borohydride solution. The sample is subjected to rotary evaporation and re-dissolved in water. Dialysis was carried out to purify the nanocomposite by making use of dialysis tubing of molecular weight cut off > 2,000.

### 2.2 Modification of Gold Substrates by Pt-dendrimer Nanocomposite

The gold disk electrode ( $\phi = 2$  mm) was mechanically polished, subjected to cleaning by cycling (15–20 cycles) between –0.4 and 1.1 V vs. Hg/Hg<sub>2</sub>SO<sub>4</sub> (MSE) in 0.5 M H<sub>2</sub>SO<sub>4</sub> and then immersed in cystamine dihydrochloride (1% solution in water) for 24 h to obtain a self assembled monolayer of cystamine. The electrode was then treated with sodium nitrite (0.05 M) and HCl (0.1 M) at 5 °C for diazotization of the amine groups of cystamine to take place. Then, the electrode was dipped in Pt-dendrimer nanocomposite for two hours when the dendrimer links covalently to the surface at 5 °C. The steps involved in preparing the dendrimer-encapsulated Pt nanoparticle film are shown in Scheme 1. The electrode, modified by the above self-assembly approach, was examined under vigorous agitation using a Rotating Disc electrode setup. The “current” responses before and after agitation were found to be the same. This shows that the modification has taken place through strong covalent linkages, resulting in the formation of a stable nanocomposite film on the electrode surface.

TEM images were recorded with a Jeol 3010 Tunneling Electron Microscope using 300 KV accelerating voltage with a 400-mesh ultrathin carbon type A copper grid. The selected area electron diffraction (SAED) was taken at an accelerating voltage at 200 KV.

Gold slides (1,000 Å gold coating on silicon wafers with an intermediate adhesion layer of 100 Å thick Ti, procured from Lance Goddard associates, USA) of size 1 × 1 cm<sup>2</sup> were used for XPS and AFM and FTIR measurements. The substrates were cleaned and modified with Pt-dendrimer nanocomposite through a base layer of cystamine, as described in Schema 1.

Atomic Force Microscopic images were recorded with the Molecular Imaging PicoSPM 2100 using gold-coated silicon nitride 30 nm cantilevers (force constant of 0.12 N/m). Samples for AFM measurements were prepared on gold slides in two different methods. In the first method, sample was prepared as per the protocol described in



**Fig. 1** TEM features of Pt–dendrimer nanocomposite

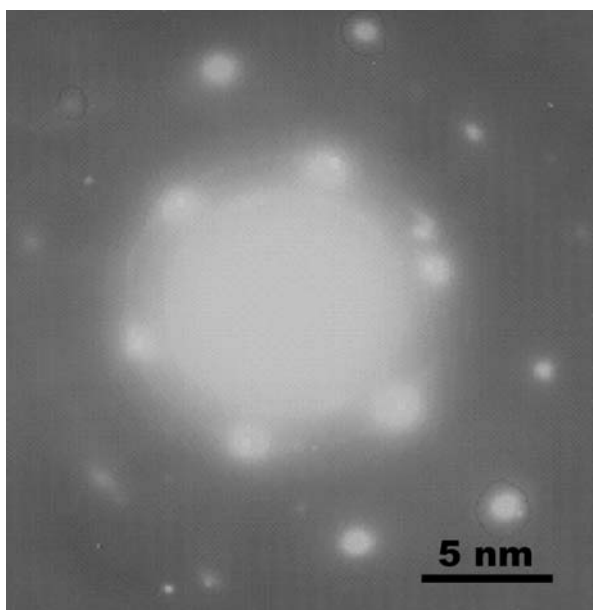
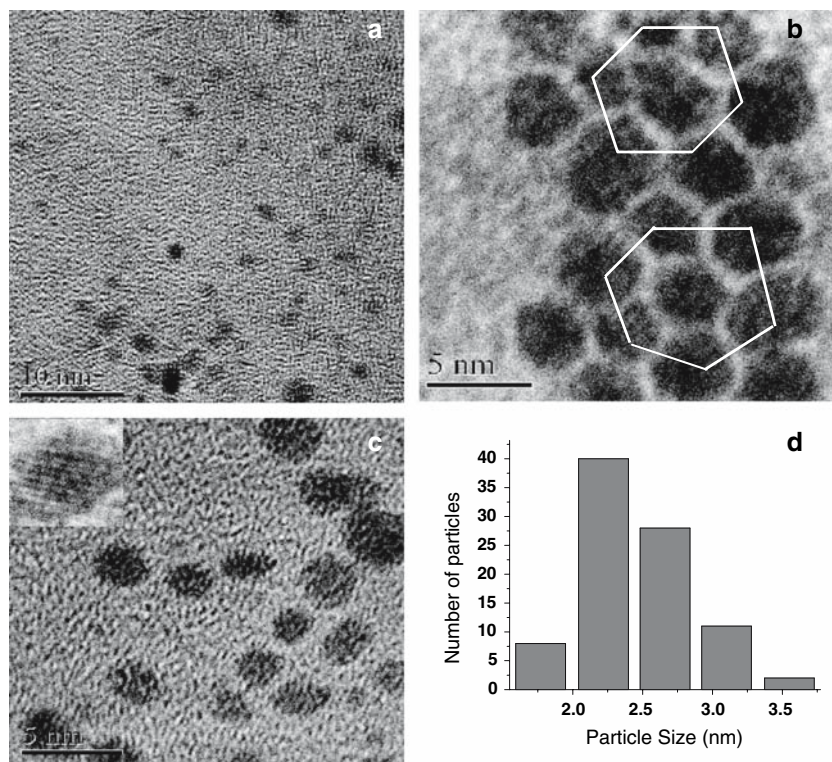


**Fig. 2** SAED pattern for Pt–dendrimer nanocomposite

crystal plane corresponding to the first circle ( $d$  value =  $2.25 \text{ \AA}$ ) was found to be (111) and that of the next circle ( $d$  value =  $1.38 \text{ \AA}$ ) to be (220). This indicates that the array formed from the nanoparticles has some long-range order suggesting preferential orientation of nanoparticles. A distinguishing feature of this work is the observation of the spot pattern with (111) single crystal

features, which has not been reported by Yang et al. [25]. However the existence of (111) planes is not seen throughout the sample. Probably a small proportion of particles are preferentially aligned. The non-uniformity of hexagonal arrangement as seen by TEM (Cf. Fig. 1) also supports the above conclusion. Moreover, the cyclic voltammetric features for  $H_{\text{upd}}$  on electrodes modified with Pt-dendrimer nanocomposite point to the presence of (111) planes (Cf. Sect. 3.4).

### 3.2 XPS and FTIR Characterization of Gold Surface Modified by Dendrimer-encapsulated Pt Nanoclusters

Many of the applications require the preparation of monodisperse nanoparticles and their attachment to solid substrates. Of particular significance is the covalent linking of nanoparticles to an electrically conducting substrate, which enables the nanoparticle array to be utilized for electrochemical applications [35]. Several surface derivatization schemes have been developed, which employ thiol, amide and related linkages and polymer/sol–gel matrices. To probe the electrochemical properties of the nanoparticle film, the anchored metal particle should “electronically” match the substrate metal. Besides, the attached nanoparticle should retain the electroactivity. Amine-terminated PAMAM and bifunctionalized PAMAM dendrimers have been linked to Au substrate through mercaptoundecanoic

acid (MUA) monolayer with and without activation by ethyl chloroformate [36, 37]. Activation by ethyl chloroformate aids the covalent linkage of dendrimers to the MUA monolayer. In the absence of activation, the dendrimer molecules are electrostatically linked to the MUA monolayer. The film resulting from covalent linkage was durable even after sonication under acidic conditions, whereas the film prepared by electrostatic attachment of the dendrimer to the mercaptoundecanoic acid (MUA) monolayer were less robust. However, there is no report about their electrocatalytic activity presumably due to the insulating SAM layer separating the Au surface from the dendrimer-encapsulated nanoparticles. The hydroxyl-terminated dendrimers were earlier linked to the glassy carbon electrodes through oxidative coupling and tested to be electrocatalytically active towards oxygen reduction [20]. In the present work, carboxyl terminated G-4.5 is loaded with Pt nanoclusters and then linked to gold surface through covalent linkages. The amine groups of the self-assembled monolayer of cystamine are diazotized and then covalently tethered to dendrimer-encapsulated Pt nanoclusters with the elimination of  $N_2$  and HCl. The linking strategy is confirmed by FTIR and surface morphology is given by AFM. The XPS measurements were done to probe the oxidation state of Pt in the modified film.

Figure 3 presents XPS results for the Au substrate modified by linking Pt-dendrimer nanocomposite to the surface through a SAM of cystamine (Cf. Scheme 1). The XP spectrum reveals the Pt nanoclusters to be in the metallic state, as seen by the peaks Pt (4f7/2) and Pt (4f5/2) appearing at 71.3 and 74.4 eV, respectively in accordance with the data reported in Ref. [38].

The FTIR spectrum obtained for the dendrimer G-4.5 evaporated on a KBr pellet is given in Fig. 4a. The bands

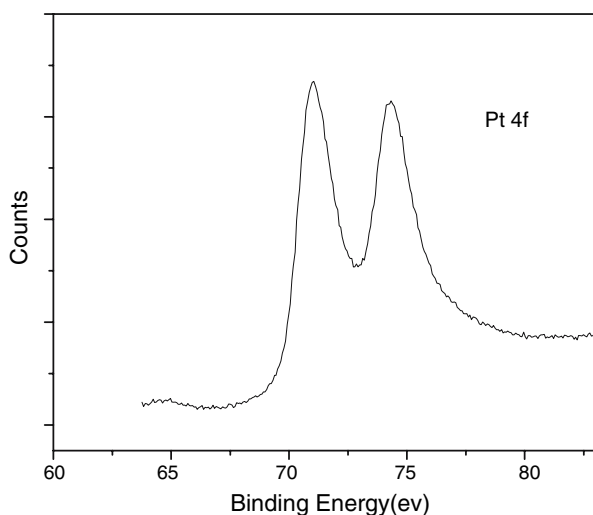
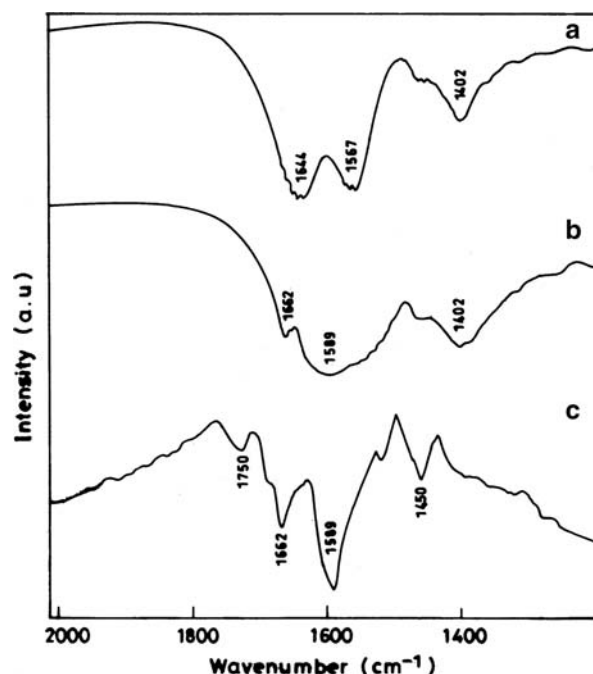


**Fig. 3** XPS response of Pt-dendrimer nanocomposite covalently linked to the gold substrate

appearing at  $1,644\text{ cm}^{-1}$ ,  $1,567\text{ cm}^{-1}$  and  $1,402\text{ cm}^{-1}$  correspond to amide I, amide II and carboxyl group, respectively. In the case of the dendrimer adsorbed physically onto gold substrate (Fig. 4b), amide I and II bands appear at  $1,662\text{ cm}^{-1}$  and  $1,589\text{ cm}^{-1}$ , respectively and the carboxyl band remains at  $1,402\text{ cm}^{-1}$ . Figure 4c presents the spectrum recorded with the gold substrate modified by Pt-dendrimer nanocomposite covalently linked through cystamine monolayer. In Fig. 4c the amide I & II bands appear at  $1,662\text{ cm}^{-1}$ ,  $1,589\text{ cm}^{-1}$  and the carboxyl band at  $1,450\text{ cm}^{-1}$ . The band at  $1,750\text{ cm}^{-1}$  confirms the presence of ester linkage between the cystamine monolayer and Pt-dendrimer nanocomposite. Compared to the case of free dendrimer (Fig. 4a) the amide I & II bands shifted to higher values in the case of Fig. 4b and c. The frequency changes noticed here may arise from the interactions between the particles and the dendrimer [13].

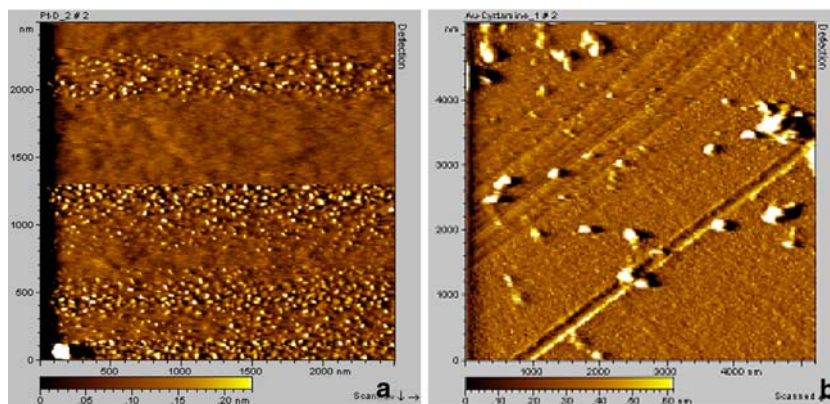
### 3.3 AFM Characterization of Gold Surface Modified by Dendrimer-encapsulated Pt Nanoclusters

Figure 5a shows the AFM image of Pt-dendrimer nanocomposite obtained by evaporation on a gold slide. The image clearly reveals the presence of nanoparticles. Similar images have been obtained earlier for samples on mica substrates [39]. Figure 5a shows that the nanoparticles are assembled together when the solvent evaporates from the surface. This is reflected by the size of the particles which



**Fig. 4** FTIR spectrum of (a) G-4.5 dendrimer (b) Pt-dendrimer nanocomposite covalently linked to the gold substrate

**Fig. 5** (a) AFM features of Pt–dendrimer nanocomposite evaporated on a gold substrate; (b) AFM features of Pt–dendrimer nanocomposite covalently linked to the gold substrate



lie mostly around 25–30 nm based on height profiles. The AFM image of the covalently bound Pt-dendrimer nanocomposite is presented in Fig. 5b. In this image, many randomly deposited globular nanoparticles are seen on the gold surface. The particles appear to be substantially uniform in size. There are a few large irregular clusters perhaps caused by dendrimer aggregation. The AFM study reveals that PAMAM G-4.5 dendrimer is an efficient host for immobilizing and stabilizing nanoclusters on gold substrates. The surface immobilization procedure, described for the first time in this work, ensures chemical linking of the platinum-loaded dendrimer to the inert electrode surface. Though the covalent bonding is weak as indicated by a weak ester band in Fig. 4, the molecules at the surface are perhaps additionally stabilized by hydrogen bonding interactions and hence the nanocomposite films are very robust.

### 3.4 Electrochemical Characterization of Pt-dendrimer Nanocomposite Modified Gold Electrodes

Figure 6 depicts the cyclic voltammograms (CV) obtained for Pt-dendrimer nanocomposite modified gold electrode in 0.1 M H<sub>2</sub>SO<sub>4</sub>. The peaks observed at –0.205 V (anodic) and –0.360 V (cathodic) is possibly due to underpotential deposition (upd) of hydrogen (H<sub>upd</sub>). To confirm the origin of the peaks, voltammetric scans were run in this potential region. These experiments revealed a linear relationship between the peak current and the scan rate ( $\nu$ ). However, the peak potential shifted to more anodic values with increasing scan rate. These peaks were found to be drawn out at  $\nu > 100$  mV/s<sup>1</sup> and the peak potential difference ( $\Delta E_p \cong |E_{pa} - E_{pc}|$ ) increased with the scan rate, showing that kinetic effect is operative. This behaviour is the typical of a reversible H<sub>upd</sub> and this arises due to the resistive nature of the film containing of the platinum nanoparticles. The response clearly shows that the Pt particles possess a preferential orientation of (111) faces [40, 41] and is supported by the SAED pattern. It is well known that, in the

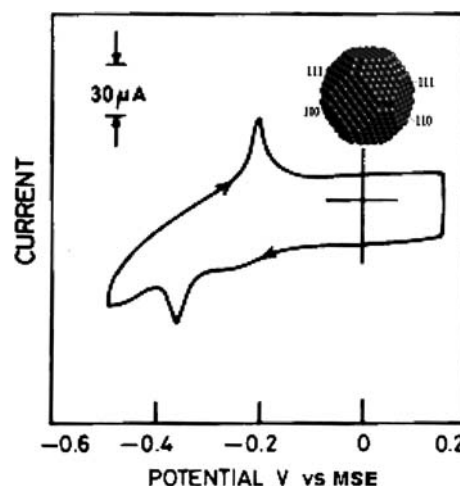


**Fig. 6** Cyclic voltammogram featuring the H<sub>upd</sub> fine structure on Pt–dendrimer nanocomposite modified gold electrode. Scan rate: 50 mV/s<sup>1</sup>. Inset: Crystal planes associated with kinks, edges and terraces of cubo-octahedron lattice of Pt

case of Pt, the near spherical nanoparticles are formed with (100) and (111) faces with numerous edges and corners and are believed to assume a cubo-octahedron structure (inset of Fig. 6) [42]. It is likely that hydrogen adsorption/desorption yields a H<sub>upd</sub> fine structure that is similar to that of Pt (111) single crystals. However, unlike the polycrystalline Pt, the upd structure is associated with a large peak separation ( $\Delta E_p$ ) between the anodic and cathodic peaks. The peak separation indicates that the Pt nanoparticles are not directly attached to the electrode surface but through a SAM of cystamine and the particles are bound inside the dendrimer. While the peak positions confirm the occurrence of H<sub>upd</sub>, the peak separation points to a resistive component due to cystamine monolayer. Peak separation and potential shifts are usually observed in the case of monolayer-covered electrodes [43]. One of the reasons why the ideal peak separation of zero is not observed is that the platinum nanoparticles within the dendrimer are connected to the electrode through a cystamine monolayer.

Monolayers usually cause peak potential separation, rendering the electron transfer sluggish and influencing the apparent rate constants of the surface confined redox species [43]. The charge under the  $H_{\text{upd}}$  peak is also higher ( $898 \mu\text{C}/\text{cm}^2$ ) compared to similar systems reported in literature, i.e.,  $210 \mu\text{C}/\text{cm}^2$  for a monolayer of hydrogen. This indicates that the dendrimer encapsulated Pt nanoclusters provide nearly four times higher surface area and holds a great promise in effecting electrochemical reactions with such high “volume-to-surface area” ratio.

At a naked Au and dendrimer-modified Au surfaces, methanol oxidation was not observed whereas at a Pt-dendrimer nanocomposite modified Au electrode, the onset of methanol oxidation occurs at a potential of about 0.46 V with a well-defined anodic peak at 0.63 V. Figure 7 shows CVs for the oxidation of methanol on Au modified with Pt-dendrimer nanocomposite. It demonstrates that the dendrimer-encapsulated Pt nanoparticles are within electron tunneling distance of the Au surface and that methanol is able to penetrate the G-4.5 dendrimer, encounter the encapsulated Pt nanoparticle, and that the product of the reaction is able to escape from the dendrimer interior. However, the oxidation potential is high (1 V vs. NHE) which is due to SAM layer and the bulky dendrimer molecule, both contributing to poor electrical communication between the electrode and the dendrimer encapsulated Pt nanoparticle. The methanol oxidation peak is broad which indicates that the methanol oxidation assisted by Pt-dendrimer nanocomposite and oxide assisted catalysis overlap. It is known that Au is a poor catalyst for the oxidation of hydrocarbons [44]. In this case, the gold electrode acts as

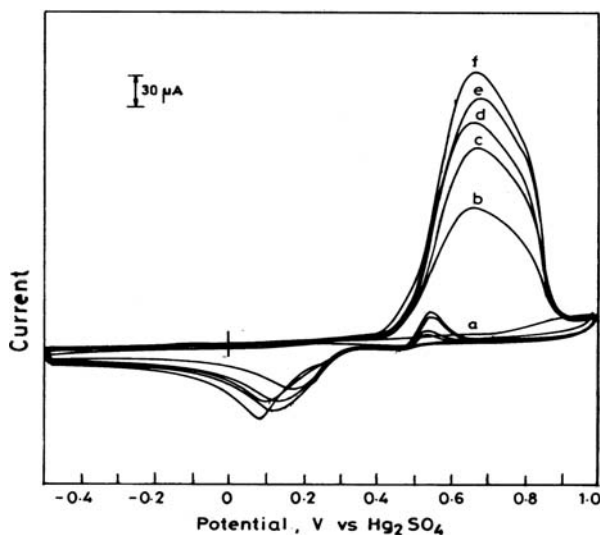


**Fig. 7** Cyclic voltammograms representing the methanol oxidation on Pt-dendrimer nanocomposite modified gold substrate for different concentrations of methanol. Scan rate:  $50 \text{ mV}/\text{s}^{-1}$  (a) 0 M; (b) 0.024 M; (c) 0.048 M; (d) 0.072 M; (e) 0.096 M; (f) 0.12 M

current collector. It can be shown in our case that the catalytic current arising due to Pt/dendrimer nanocomposite and platinum oxide/dendrimer nanocomposite can be clearly resolved (Fig. 8a–c). Figure 8a–c represent the oxidation of methanol, ethanol and ethylene glycol on Pt-dendrimer nanocomposite electrode. In all the cases the peak 1 correspond to the oxidation of the substrate catalysed by Pt and peak 2 correspond to oxide assisted catalysis.

A critical assessment of the above results on methanol electrooxidation highlights the following observations that deserve to be contrasted with the behaviour noticed at a polycrystalline Pt surface. At the Pt-dendrimer nanocomposite modified electrode, there is very little current in the reverse scan unlike in the case of polycrystalline Pt. More importantly, repeated cycling in this potential region does not affect the current response and the observed peak currents increase with increase in the concentration of methanol. This may be compared with the results of Park et al. [45] employing carbon-supported Pt nanoparticles, wherein the currents did not increase greatly when methanol concentration was changed from 0.01 to 0.1 M. Their observations with 2.2 nm sized Pt/C indicate only intermediate CO coverage with methanol dosing.  $\theta_{\text{CO}}$  becomes lower as the size of the particles becomes smaller. They concluded that this was indicative of an apparent limitation in the availability of catalytic surface sites (geometric effect). It may also be recalled that Pt (111) terraces facilitate oxidative removal of CO [45]. In addition, if  $\text{CO}_2$  formation requires a smaller ensemble than does CO formation, then  $\text{CO}_2$  production will be favoured even at a small CO coverage. In this case, CO acts as both poison and promoter. While the inherently high surface area associated with Pt-dendrimer nanocomposite (indicated by the  $H_{\text{upd}}$  charge) is responsible for the enhanced catalytic activity of the dendrimer-Pt nanocomposite, it is also conjectured that the enhanced catalytic activity noticed in our case may also arise from the increase in the proportion of terrace sites (111) that facilitate the oxidative removal of  $\text{CO}_{\text{ads}}$  [46, 47]. An insignificant anodic peak observed on scan reversal precludes the possibility of the catalytic activity arising from roughness factor during potential excursions into the anodic region. The oxidation currents observed in the case of methanol, ethanol and ethylene glycol are given in Table 1. The results shown here were reproducible for many experiments run after the electrode was left open to air for a few days. This not only demonstrates the reproducibility of the results but also the stability of the nanoparticles.

Compared to the results [48] of the oxidation of methanol, ethanol and ethylene glycol on a polycrystalline Pt electrocatalyst, the catalytic currents noticed in this study are significantly higher even in low concentrations of methanol, thereby indicating the high catalytic activity of our Pt-dendrimer nanocomposites. Typically, our modified

**Fig. 8** Cyclic voltammogram representing the oxidation of small molecules (**A**-Methanol, **B**-Ethanol, **C**-Ethylene Glycol) on Pt–dendrimer nanocomposite modified gold substrate for different concentrations of the substrate. Scan rate:  $50 \text{ mV/s}^{-1}$  (a) 0 M; (b) 0.024 M; (c) 0.048 M; (d) 0.072 M; (e) 0.096 M; (f) 0.12 M (In the case of Ethylene glycol only two additions are represented)

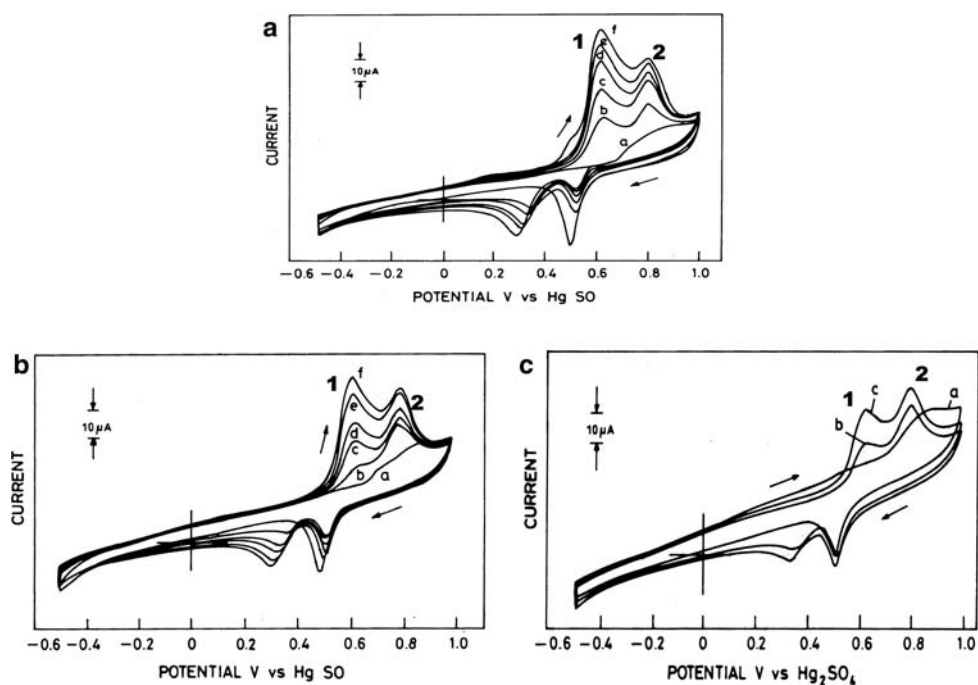


**Table 1** Voltammetric oxidation peak characteristics of the alcoholic fuels

Methanol		Ethanol		Ethylene glycol	
Concentration (M)	Oxidation peak current density ( $\mu\text{A}/\text{cm}^2$ )	Concentration (M)	Oxidation peak current density ( $\mu\text{A}/\text{cm}^2$ )	Concentration (M)	Oxidation peak current density ( $\mu\text{A}/\text{cm}^2$ )
0.024	$39 \times 10^2$	0.017	$15 \times 10^2$	0.017	$6 \times 10^2$
0.048	$56 \times 10^2$	0.034	$27 \times 10^2$	0.035	$18 \times 10^2$
0.072	$64 \times 10^2$	0.051	$37 \times 10^2$	0.054	$20 \times 10^2$
0.096	$72 \times 10^2$	0.068	$44 \times 10^2$	0.071	$29 \times 10^2$
0.120	$80 \times 10^2$	0.085	$55 \times 10^2$	0.090	$32 \times 10^2$

electrode yields for the oxidation of methanol and ethanol, peak current density values that are about one order higher than those obtained on polycrystalline electrode of same geometric surface area. In the case of ethylene glycol also, a similar trend is noticed and the current density enhancement is about two times. It is interesting to recall [45] that such an enhancement in activity could not be noticed in the methanol oxidation peak current density for the polycrystalline versus nanoparticle electrodes. In other words, the present results confirm the catalytic efficacy of the modification described in this work. This would finally lead to a lower catalyst loading in the electrodes employed in fuel cells or other electrochemical devices. The enhancement in catalytic activity must result from the nanostructured nature of the platinum particles. However, at the dendrimer-modified electrode, the onset of oxidation potential is found shifted anodically. This may be attributed to the resistance offered by the SAM layer, which

could be responsible for the observed  $\Delta E_p$  values greater than zero in the case of  $\text{H}_{\text{upd}}$ .

#### 4 Conclusion

The spectral and electrochemical investigations reported in this study clearly demonstrate the possibility of immobilizing dendrimer-encapsulated Pt nanoparticles onto an electrode surface by linking it through a cystamine monolayer self assembled on a gold electrode. The novel linking strategy presented in this work while affording robust electrochemically active and catalytic thin films, also overcomes the limitation [14] of films prepared by electrostatic attachment of the dendrimer to the MUA monolayer. The significant findings of the study are: (1) carboxyl-terminated Generation 4.5 dendrimer has been shown as an effective template for encapsulating Pt nanoparticles; (2) dendrimer-encapsulated Pt nanoparticles are

tethered to gold electrodes through a SAM layer of cystamine, which is diazotized and then linked to the carboxyl group of the dendrimer. This method of modification yields binding through an ester linkage as evidenced by the FTIR observations. (3) TEM and XPS measurements clearly demonstrate that the modification protocol yields near monodisperse Pt nanoparticles neatly trapped inside the dendrimer. The existence of Pt(111) planes in the nanocomposite is confirmed by SAED and electrochemical measurements. (4) The studies further reveal the electrocatalytic activity of the modified electrode for the oxidation of small organics such as methanol, ethanol and ethylene glycol. Cyclic voltammetry of methanol electrooxidation demonstrates that the dendrimer-encapsulated Pt nanoparticles are within the electron tunneling distance of the Au surface and that methanol is able to penetrate the G-4.5 dendrimer, encounter the encapsulated Pt nanoparticle, and that the product of the reaction is able to escape from the dendrimer interior. Repeated cycling in the potential region of methanol oxidation does not affect the current response showing the stability of the modification. (5) In significant contrast to the results of the oxidation of methanol on carbon-supported Pt nanoparticle films [22], the present investigations show distinct catalytic activity of the modified electrode even at very low concentrations of methanol, possibly arising from the increased proportion of terrace sites (111) generated by this novel modification procedure. Selected area electron diffraction, in conjunction with the  $H_{\text{upd}}$  fine structure confirms the formation of Pt nanoparticles oriented in (111) direction according to a cubo-octahedron structure model.

In our *as yet* unpublished work, the modification protocols described in this study have also been found to facilitate the incorporation of bimetallic nanoclusters, thereby offering versatility and scope to design effective electrocatalysts, especially in the context of microfuel cells and “dendri-chips” [49]. Materials of high *surface-to-volume* ratios that can be generated using particles encapsulated within dendrimer matrices are more suitable for miniaturized electrochemical systems, especially when platforms like *micro-total analytical systems* are involved.

**Acknowledgments** Authors thank the Water & Steam Laboratory, IGCAR for XPS, and SAIF (IIT-Mumbai) and JNCASR, Bangalore for TEM measurements. The financial support by DRDO & DST (New Delhi) for the projects on Nanoscale Materials is gratefully acknowledged.

## References

- Raimondi F, Scherer GG, Katz R, Wokaun A (2005) *Angew Chem Int Ed* 44:2190
- Peng X, Koczur K, Nigro S, Chen A (2004) *Chem Commun* 2872
- Zhou ZH, Wang S, Zhou W, Wang G, Jiang L, Li W, Song S, Liu J, Sun G, Xin Q (2003) *Chem Commun* 394
- Chan K-Y, Ding J, Ren J, Cheng S, Tsang KY (2004) *J Mater Chem* 14:504
- Park S, Chung TD, Kim HC (2003) *Anal Chem* 75:3046
- Scott RWJ, Wilson OM, Crooks RM (2005) *J Phys Chem B* 109:692
- Crooks RM, Zhao M, Sun L, Chechik V, Yeung LK (2001) *Acc Chem Res* 34:181
- Zhao M, Sun L, Crooks RM (1998) *J Am Chem Soc* 120:4877
- Niu Y, Yeung LK, Crooks RM (2001) *J Am Chem Soc* 123:6840
- Li Y, El-Sayed MA (2001) *J Phys Chem B* 105:8938
- Rahim EH, Kamounah FS, Frederiksen J, Christensen JB (2001) *Nano Lett* 1:499
- Ooe M, Murata M, Mizugaki T, Ebitani K, Kaneda K (2002) *Nano Lett* 2:999
- Manna A, Imae T, Aoi K, Okada M, Yogo T (2001) *Chem Mater* 13:1674
- Chung Y-M, Rhee H-K (2003) *Catal Lett* 85:159
- Toshima N, Yonezawa T, Kushihashi K (1993) *J Chem Soc Faraday Trans* 89:2537
- Scott RWJ, Datye AK, Crooks RM (2003) *J Am Chem Soc* 125:3709
- Scott RWJ, Wilson OM, Oh S-K, Kenik EA, Crooks RM (2004) *J Am Chem Soc* 126:15583
- Ledesma-Garcia J, Manriquez J, Gutierrez-Granados S, Godinez LA (2003) *Electroanalysis* 15:659
- Bustos E, Manriquez J, Orozco G, Godinez LA (2005) *Langmuir* 21:3013
- Ye H, Crooks RM (2005) *J Am Chem Soc* 127:4930
- Esumi K, Akiyama S, Yoshimuna T (2003) *Langmuir* 19:7679
- Esumi K, Houdatsu H, Yoshimura T (2004) *Langmuir* 20:2536
- Endo T, Yoshimura T, Esumi K (2005) *J Colloid Interface Sci* 286:602
- Esumi K, Suzuki A, Yamahira A, Torigoe K (2000) *Langmuir* 16:2604
- Yang L, Luo Y, Jia X, Ji Y, You L, Zhou Q (2004) *J Phys Chem B* 108:1176
- Kim JW, Choi E-A, Park S-M (2003) *J Electrochem Soc* 150:E202
- Raghu S, Berchmans S, Phani KLN, Yegnaraman V (2005) *Pramana J Phys* 65:821
- McMurray J (2000) *Organic chemistry*, 5th edn. Brooks/Cole, USA, p 895, 1003
- Gröhn F, Bauer BJ, Akpalu YA, Jackson CL, Amis EJ (2000) *Macromolecules* 33:6042
- Prosa TJ, Bauer BJ, Amis EJ, Tomalia DA, Scherrenberg R (1997) *J Polym Sci* 35:2913
- Left DV, Ohara PC, Heath JR, Gelbert WM (1995) *J Phys Chem* 99:7036
- Diallo MS, Christie S, Swaminathan P, Balogh L, Shi X, Um W, Papelis C, Goddard WA III, Johnson JH Jr (2004) *Langmuir* 20:2640
- Maiti PK, Cagin T, Lin ST, Goddard WA III (2006) *Macromolecules* 38:979
- Ottaviani MF, Bossmann S, Turro NJ, Tomalia DA (1994) *J Am Chem Soc* 116:661
- Park S, Weaver MJ (2002) *J Phys Chem B* 106:8667
- Ye H, Scott RWJ, Crooks RM (2004) *Langmuir* 20:2915
- Oh S-K, Kim Y-G, Ye H, Crooks RM (2003) *Langmuir* 19:10420
- Zhao M, Crooks RM (1999) *Adv Mater* 11:217
- Gu Y, Xie H, Gao J, Liu D, Williams CT, Murphy CJ, Ploehn HJ (2005) *Langmuir* 21:3122
- Bard AJ, Faulkner LR (2001) *Electrochemical methods*, 2nd edn. John Wiley & Sons Inc., NY, p 560

41. Kabbabi A, Gloaguen F, Andolfatto F, Durand RJ (1994) *J Electroanal Chem* 373:251
42. Attard GA, Ahmadi A, Jenkins DJ, Hazzazi OA, Wells PB, Griffin KG, Johnson P, Gillies JE (2003) *Chem Phys Chem* 4:123
43. Finklea HO (1996) In: Bard AJ, Rubinstein J (eds) *Electroanalytical chemistry*, vol 19. Marcel Dekker, New York, pp 109–335
44. Bond GC (2002) *Catal Today* 72:5
45. Park S, Xie Y, Weaver MJ (2002) *Langmuir* 18:5792
46. Jarvi TD, Stuve EM (1998) In: Lipkowsky J, Ross PN (eds) *Electrocatalysis, frontiers of electrochemistry series*, Chapter 3. Wiley-VCH Publishers, New York, pp 75–153
47. Mukerjee S, McBreen J (1998) *J Electroanal Chem* 448:163
48. Casado-Rivera E, Volpe DJ, Alden L, Lind C, Downie C, Vazquez-Alvarez T, Angelo ACD, DiSalvo FJ, Abruna HD (2004) *J Am Chem Soc* 126:4043
49. Nierengarten J-F (2005) *Angew Chem Int Ed* 44:2830